

Multimodal Sparse Representation-Based Classification Scheme for RF Fingerprinting

Kiwon Yang¹, Jusung Kang, Jehyuk Jang¹, and Heung-No Lee¹, *Senior Member, IEEE*

Abstract—In this letter, we propose a multimodal method for improving radio frequency (RF) fingerprinting performance that uses multiple features cultivated from RF signals. Combining multiple features, including a falling transient feature that has not previously been used in RF fingerprinting studies, we aim to demonstrate that the proposed method results in improved accuracy. We show that a sparse representation-based classification (SRC) scheme can be a good platform for combining multiple features. The experimental results on RF signals acquired from eight walkie-talkies show that the RF fingerprinting accuracy of the proposed method improves significantly as the number of features increases.

Index Terms—Classification algorithm, feature extraction, multimodality, RF fingerprinting, radio frequency identification.

I. INTRODUCTION

CLASSIFYING radio frequency (RF) signals is useful in electronic warfare to identify the radio transmission signals of adversaries [1]. For the classification to work well, the availability of good features and a simple but robust technique are essential. A feature is a sample vector cultivated from the transmitted RF signals and bears unique information about the pertinent device. Identification of RF transmitters using such features is called RF fingerprinting. Features are known to arise from many sources, including tiny differences in device fabrication process and electronic components [1].

RF fingerprinting has attracted significant attention [2]–[6]: In [2], RF-DNA features which contain information on variance, skewness, and kurtosis, within a preamble response were used with an ensemble method. In [3], four features—differential constellation trace figure, carrier frequency offset, modulation offset, and I/Q offset where classifications were done by calculating the minimum distance between test data and training data—were used. In [4], the mean of the instantaneous amplitude of the received signal and the modulation symbol were used with an optimal dimension-reduced matrix. In [5], an RF fingerprinting scheme based on low-rank representation of the original data with the robust classifier parameter was investigated. In [6], a convolutional neural network (CNN) for seven commercial Zigbee devices was used. They

collected 1,000 data per class. In [2]–[6], RF fingerprinting schemes with multiple features, which exhibited a high accuracy rate, were proposed for Zigbee devices and satellite terminals.

The contributions and novelties of this letter are as follows:

- We propose a new RF fingerprinting algorithm and a set of three RF features—*rising transient*, *falling transient*, and *sync*—and show the possibility that each feature can provide unique information through a real-life experiment. The falling transient feature has never been used in RF fingerprinting studies. Our results indicate that the performance of RF fingerprinting improves as each feature is additionally employed.
- Even though SRC is a common algorithm in classification [7], no study on RF fingerprinting with a combination of SRC and multiple features has been reported. We show that SRC can be a good platform for RF fingerprinting.

The remainder of this letter is organized as follows. The experimental system is described in Section II. The proposed method is outlined in Section III. Results are presented and analyzed in Section IV. The conclusion is given in Section V.

II. EXPERIMENTAL SYSTEM

A. Walkie-Talkie Signals

Our RF signals follow the digital mobile radio (DMR) standard. The DMR standard follows time-division multiple access (TDMA) and 4-level frequency-shift keying modulation [8]. A signal burst appears for 30ms and disappears for 30ms using the 2-slot TDMA method. This pattern is repeated in transmission.

The signal burst consists of rising transient, falling transient, and steady-state signals. The rising transient signal grows from zero to the designed level of the RF signal. Contrary to the rising transient signal, the falling transient signal decreases from the designed level to zero. The steady-state signal refers to the resting part between the rising and the falling transient signal and is composed of data and a sync signal. The data have 216 bits and the sync signal has 48 bits. The bit rate of the DMR standard is 9,600 bits/s. The sync signal is used to synchronize the transmitter and receiver.

From the pertinent signal part, a feature is obtained. Each feature is the main lobe of a spectrum of the pertinent signal part. We show how to extract each feature from the pertinent signal part in Section III. A. As we mentioned, the features arise from the inherent nonlinear properties of radio transmitters in the manufacturing process [1]. Owing to the presence of such features, RF fingerprinting can be accomplished.

Manuscript received December 24, 2018; revised January 31, 2019; accepted February 28, 2019. Date of publication March 20, 2019; date of current version May 8, 2019. This work was supported by the National Research Foundation of Korea (NRF) grant funded by the Korean government (MSIP) (NRF-2018R1A2A1A19018665). The associate editor coordinating the review of this letter and approving it for publication was F. Wang. (*Corresponding author: Heung-No Lee.*)

The authors are with the School of Electrical Engineering and Computer Science, Gwangju Institute of Science and Technology, Gwangju 61005, South Korea (e-mail: heungno@gist.ac.kr).

Digital Object Identifier 10.1109/LCOMM.2019.2905205

B. Signal-Acquisition Setup

For our experiment, two walkie-talkie models were used: Motorola *SIIM* and Hytera *BD-358*. Each model follows the DMR standard. Four units of each type, i.e., eight walkie-talkies in total, were used in the experiment.

Signal was transmitted from the transmitter and acquired from an SMA male mini car-mounted antenna, the receiving frequency band of which is 400–470 MHz. We then down-converted 423.1875 MHz to 10 MHz using an XL-11-411 RF mixer and an E4438C ESG vector signal generator. Then, we filtered the signal bandwidth and sampled the signal using an IF recording system with the PX14400 operator functioning as a low-pass filter and analog-to-digital converter. Signals sampled at 96 MHz were saved to a computer and loaded to MATLAB. As we captured 50 signals per walkie-talkie, 400 signals were saved to the computer.

III. PROPOSED FEATURE EXTRACTION AND CLASSIFICATION

A. Signal Burst to Features

To cultivate features, we extracted the three signal parts from a single signal burst. Then, each feature was selected from the pertinent extracted signal parts.

Each signal part is extracted from the first signal burst of the total received signal through time-windowing. To design the time-window for each signal, we used a thresholding method. For a rising transient signal $\mathbf{f}_R \in \mathbb{R}^{500,000 \times 1}$, the starting threshold is the first time point at which the amplitude of the signal burst exceeds 10% of its maximum; the ending threshold is the time point it exceeds 90%. Similarly, for the falling transient signal $\mathbf{f}_F \in \mathbb{R}^{500,000 \times 1}$, the starting threshold and the ending threshold are the latest time points at which the amplitude of the signal burst exceeds 90% and 10% of its maximum, respectively. Since the length of each transient signal fluctuates, we used zero padding method after the ending point of each transient signal to match the length. To design the time window for the sync signal, we referred to the DMR standard [8]. The sync signal $\mathbf{f}_S \in \mathbb{R}^{480,000 \times 1}$ is located at the center of a signal burst. We set the center of the time-window for the sync signal to the central time point between the ending time of the rising transient signal and the starting time of the falling transient signal. The width of the time window was set to 0.005 s, as per the DMR standard [8]. Each extracted signal part was normalized to consider the case of signals with different power levels.

The extracted signal parts were transformed to the spectrum domain by fast Fourier transform (FFT) with the size of the time signal. Then, the operation of taking the absolute value of each element was executed to compare the energy and frequency information of the extracted signal part with those of the others. Since the main lobe occupies most of the energy of each signal part, the main lobe was taken from each spectrum. The main lobes, $F(\mathbf{f}_R)_{ML} \in \mathbb{R}^{2,000 \times 1}$, $F(\mathbf{f}_F)_{ML} \in \mathbb{R}^{2,000 \times 1}$, and $F(\mathbf{f}_S)_{ML} \in \mathbb{R}^{1,920 \times 1}$, are the unique features used in our experiment, where $F(\cdot)$ is the FFT operation function and ML denotes the main lobe of the spectrum.

To extract the main lobe, we used a bandpass filter first. Then, the center frequency of the filtered spectrum was down-converted to zero. Finally, we decimated the signal to reduce the length of the sample sequence. The main lobe was set to occupy most of the energy of each signal part, considering the channel bandwidth.

B. Proposed SRC

SRC is a classification algorithm based on the compressed sensing theory [7] and is used to determine the class from the sparse solution of the representation equation

$$\mathbf{y} = \mathbf{D}\mathbf{s}, \quad (1)$$

where $\mathbf{y} \in \mathbb{R}^{P \times 1}$ is a test data vector with length P , $\mathbf{D} \in \mathbb{R}^{P \times NL}$ is a training data matrix composed of N training data vectors for each class label of transmitters $l \in \{1, \dots, L\}$, and $\mathbf{s} \in \mathbb{R}^{NL \times 1}$ is a vector of sparse representation coefficients. The sparse signal recovery algorithm in [7] was used to solve (1) with $P < NL$. In (1), $\mathbf{D}\mathbf{s}$ can be rewritten as

$$\mathbf{D}\mathbf{s} = [\mathbf{D}^{(1)} \quad \dots \quad \mathbf{D}^{(L)}] \left[(\mathbf{s}^{(1)})^T \quad \dots \quad (\mathbf{s}^{(L)})^T \right]^T, \quad (2)$$

where $\mathbf{D}^{(l)}$ is a submatrix of \mathbf{D} corresponding to the l^{th} class label of transmitters and $\mathbf{s}^{(l)}$ is a subvector of \mathbf{s} corresponding to the l^{th} class label of transmitters, and T denotes the transpose. To identify the class of test data, we solve

$$\text{class} = \arg \min_{l \in \{1, \dots, L\}} \left\| \mathbf{y} - \mathbf{D}^{(l)} \mathbf{s}^{(l)} \right\|_2. \quad (3)$$

If the column vectors in \mathbf{D} are less correlated, the solution \mathbf{s} of (1) is approximated to be sparse since the condition of having a sparse solution depends on the mutual correlation between the columns of \mathbf{D} [9]. Thus, the compressed sensing algorithms in [7] can be used to find a unique solution \mathbf{s} . However, when RF signals are taken directly to form the column vectors of \mathbf{D} , the solution \mathbf{s} cannot be sparse because they may be highly correlated. Then, the performance of SRC may be poor. Thus, RF signals must be processed to remove correlation to obtain high performance in SRC [9].

To remove correlation among RF signals, the proposed method applies principal components analysis (PCA) to the column vectors, each of which combines multiple features. PCA is known to be good at geometrically separating the features in the Euclidean domain by removing the mutual correlation [10]. This section aims to show how three kinds of features are concatenated and how PCA is applied to the features. We first introduce the single modal method and then discuss the proposed multimodal method.

1) *Single Modal RF Fingerprinting*: Consider that one of the rising transient, falling transient, and sync features is used as the sole representative feature of a single transmitter. We first form a feature matrix in which the columns are the sample vectors of the feature of candidate RF transmitters. Mathematically, for L RF transmitters (classes) and N sample vectors of a feature of each RF transmitter, we construct the feature matrix $\mathbf{A} \in \mathbb{R}^{M \times NL}$ as follows:

$$\mathbf{A} = \left[\mathbf{a}_1^{(1)}, \dots, \mathbf{a}_N^{(1)}, \mathbf{a}_1^{(2)}, \dots, \mathbf{a}_N^{(L)} \right], \quad (4)$$

where column vector $\mathbf{a}_n^{(l)} \in \mathbb{R}^{M \times 1}$ is the n^{th} sample vector of a feature of the l^{th} RF transmitter for $n = 1, \dots, N$ and $l = 1, \dots, L$, and M is the length of a feature. We denote a feature of an unknown RF transmitter as $\mathbf{u} \in \mathbb{R}^{M \times 1}$. From the PCA operation, (7) and (9), \mathbf{A} and \mathbf{u} are changed to a training data matrix \mathbf{D} and a test data vector \mathbf{y} , respectively.

2) *Multimodal RF Fingerprinting*: The proposed method is to concatenate the multiple features in the representation equation $\mathbf{u} = \mathbf{A}\mathbf{s}$, as shown in Fig. 1; the feature matrices are concatenated in a row-wise manner. Let us denote the n^{th} sample vector of the k^{th} feature of the l^{th} RF transmitter for $n = 1, \dots, N$, $l = 1, \dots, L$, and $k = 1, \dots, K$ as $\mathbf{a}_{k,n}^{(l)} \in \mathbb{R}^{M \times 1}$, where K is the number of features to be combined. The feature matrices are concatenated as follows:

$$\mathbf{A} = [\mathbf{A}_1^T \quad \mathbf{A}_2^T \quad \dots \quad \mathbf{A}_K^T]^T \in \mathbb{R}^{MK \times NL}, \quad (5)$$

where $\mathbf{a}_{k,n}^{(l)}$ forms the columns of feature matrix \mathbf{A}_k ,

$$\mathbf{A}_k = [\mathbf{a}_{k,1}^{(1)}, \dots, \mathbf{a}_{k,N}^{(1)}, \mathbf{a}_{k,1}^{(2)}, \dots, \mathbf{a}_{k,N}^{(L)}] \in \mathbb{R}^{M \times NL}. \quad (6)$$

Then, PCA is applied to the feature matrix \mathbf{A} . We obtain the training data matrix \mathbf{D} as follows:

$$\mathbf{D} = \mathbf{V}^T(\mathbf{A} - \mathbf{m}\mathbf{1}) \in \mathbb{R}^{P \times NL}, \quad (7)$$

where $\mathbf{m} = \frac{1}{L \times N} \sum_{l=1}^L \sum_{n=1}^N \mathbf{a}_n^{(l)} \in \mathbb{R}^{MK \times 1}$ is the average vector of the columns of \mathbf{A} , $\mathbf{1} := [1 \ 1 \ \dots \ 1]$ is the 1 by NL vector of 1s, $\mathbf{a}_n^l = [(\mathbf{a}_{1,n}^{(1)})^T (\mathbf{a}_{2,n}^{(1)})^T \dots (\mathbf{a}_{K,n}^{(L)})^T]^T \in \mathbb{R}^{MK \times 1}$ is a column vector which combines K features, and $\mathbf{V} \in \mathbb{R}^{MK \times P}$ is a rearranged eigenvector matrix of the covariance matrix $(\mathbf{A} - \mathbf{m}\mathbf{1})(\mathbf{A} - \mathbf{m}\mathbf{1})^T \in \mathbb{R}^{MK \times MK}$. The eigenvectors of $(\mathbf{A} - \mathbf{m}\mathbf{1})(\mathbf{A} - \mathbf{m}\mathbf{1})^T$ are arranged according to the eigenvalues in descending order. Since the eigenvalue of the covariance matrix is proportional to the variance of the columns of \mathbf{A} and the eigenvectors of the covariance matrices are orthonormal, the column vector of \mathbf{V} becomes a basis of the new space on the variance of the columns of \mathbf{A} [10]. The dimension of \mathbf{V} can be selected by the user as $P \in \{1, \dots, MK\}$. To obtain the test data vector \mathbf{y} of SRC, we first concatenate different features of an unknown transmitter $\mathbf{u}_k \in \mathbb{R}^{M \times 1}$ as follows:

$$\mathbf{u} = [\mathbf{u}_1^T \quad \mathbf{u}_2^T \quad \dots \quad \mathbf{u}_K^T]^T \in \mathbb{R}^{MK \times 1}. \quad (8)$$

Finally, PCA is applied to a concatenated feature of unknown transmitter \mathbf{u} . The test data vector \mathbf{y} is obtained by mapping the difference between concatenated feature \mathbf{u} and \mathbf{m} , i.e., $\mathbf{u} - \mathbf{m}$, onto the space with the eigenvector matrix \mathbf{V} ,

$$\mathbf{y} = \mathbf{V}^T(\mathbf{u} - \mathbf{m}) \in \mathbb{R}^{P \times 1}. \quad (9)$$

By using PCA, the equation in Fig. 1 is changed to (1), which has principal components as training and test data. The SRC solution in (1) was determined using the basis pursuit algorithm, which finds the unique sparse solution that has the minimum L1 norm [11].

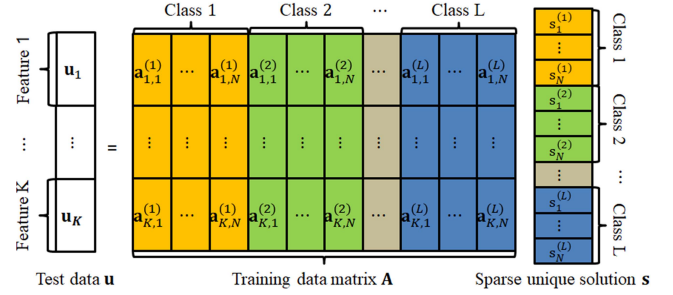


Fig. 1. Feature concatenation in the proposed method.

TABLE I
ACCURACY RATE OF THE PROPOSED METHOD

	4 BD-358	4 SLIM	4 BD-358 4 SLIM
Accuracy rate (Minimum number of PC)			
TR(R)	88% (24)	82% (48)	90.5% (45)
TR(F)	87.5% (45)	90% (12)	92.25% (13)
TR(R + F)	93% (49)	92% (20)	95.5% (63)
Sync	99% (45)	83.5% (22)	93.75% (86)
TR(R + F) + Sync	99% (44)	98.5% (22)	98.75% (21)

R: Rising, F: Falling, PC: Principal components

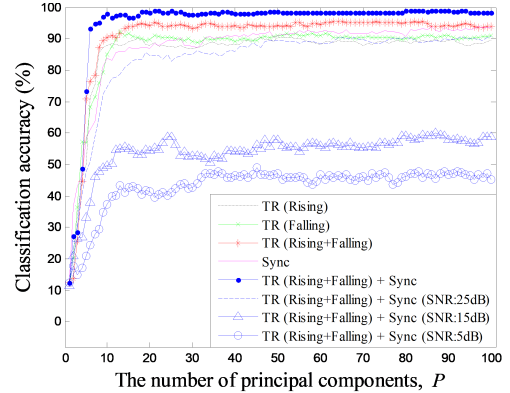


Fig. 2. Classification result of four BD-358 and four SLIM walkie-talkies.

IV. EXPERIMENTAL RESULTS AND DISCUSSION

For our experiment, we set the decimation rate for all feature extractions to 250, considering the bandwidth of the RF signal following the DMR standard [8] and the sampling rate. To evaluate the performance of the proposed classifier, we used a five-fold cross validation technique. Fifty data were used per walkie-talkie, such that each test data was classified on the total of 320 training data. The experiment was performed in a line-of-sight environment and SNR was around 35-40 dB.

Table I shows the accuracy rate of the proposed method. The accuracy rate of the multimodal scheme is much better than that obtained from using only one feature. The minimum number of principal components is the minimum number of column vectors in the eigenvector matrix \mathbf{V} that yields the highest accuracy rate. Fig. 2 shows eight results of classification using 1 to 100 principal components, 1) on the rising transient feature, 2) on the falling transient feature, 3) on both transient features combined, 4) on the sync feature, and

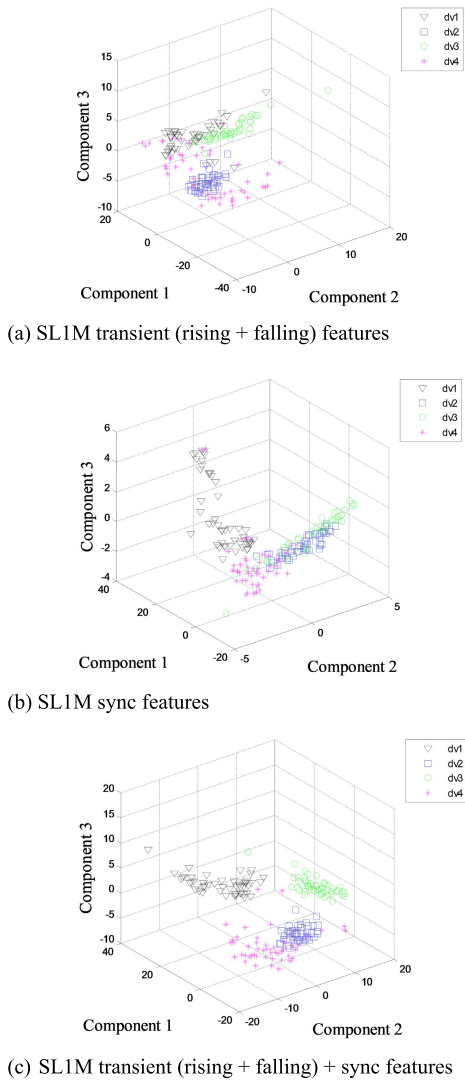


Fig. 3. Feature map of a 3-D principal components space.

5) on all features combined in SNR : 35-40dB, 6) 25dB, 7) 15dB, and 8) 5dB. Improved performance with an increased number of features indicates that each feature could contain unique information. Since the eigenvectors of the 21st and higher eigenvalues of $(\mathbf{A} - \mathbf{m}\mathbf{1})(\mathbf{A} - \mathbf{m}\mathbf{1})^T$ do not have enough information to represent the differences of data, the classification accuracy is not changed as $P > 21$. Fig. 3 shows a feature map in which the principal components of features of Motorola *SLIM* are mapped onto a 3D plot. The label of each axis, such as Component 1 and Component 2, means the projection of $\mathbf{u} - \mathbf{m}$ to the P^{th} column vector of \mathbf{V} . The figure shows distinct cluster formation when a concatenated feature is used.

To compare the proposed method with convolutional neural network (CNN), we referred to the studies [6] and [12]. For additional tests, we used a five-fold cross validation technique. Five training neural networks were constructed

using the same training dataset with the proposed method. We used the concatenated features as input data. The average classification accuracy rate of the CNN was 91.5%.

In our experiment, the size of the training data set is much smaller than that of [6]. Comparing CNN (91.5%) with the proposed method (98.75%), we show that SRC performs better than CNN for this small training data set. Because it is simple to add more training data and different kinds of features in SRC, the performance of the proposed method could be improved with additional training data and other kinds of features.

V. CONCLUSIONS

This letter proposed a multimodal RF fingerprinting scheme based on SRC. We showed that the proposed multimodal scheme, which concatenates multiple features in the row-wise manner and applies PCA to the concatenated dictionary matrix, improves accuracy significantly. We showed the possibility that the three signal features we have cultivated from RF signal samples could provide mutually independent information. The proposed scheme is efficient in the sense that improved RF fingerprinting accuracy is obtained. In addition, it is simple and easy in the proposed scheme to add more data and various kinds of features. The MATLAB source code for this study can be obtained at https://infonet.gist.ac.kr/?page_id=14.

REFERENCES

- [1] Y. Jia, S. Zhu, and L. Gan, "Specific emitter identification based on the natural measure," *Entropy*, vol. 19, no. 3, p. 117, 2017.
- [2] H. J. Patel, M. A. Temple, and R. O. Baldwin, "Improving ZigBee device network authentication using ensemble decision tree classifiers with radio frequency distinct native attribute fingerprinting," *IEEE Trans. Rel.*, vol. 64, no. 1, pp. 221–233, Mar. 2015.
- [3] L. Peng, A. Hu, J. Zhang, Y. Jiang, J. Yu, and Y. Yan, "Design of a hybrid RF fingerprint extraction and device classification scheme," *IEEE Internet Things J.*, vol. 6, no. 1, pp. 349–360, Feb. 2019.
- [4] Y. Jia, J. Ma, and L. Gan, "Combined optimization of feature reduction and classification for radiometric identification," *IEEE Signal Process. Lett.*, vol. 24, no. 5, pp. 584–588, May 2017.
- [5] Y. Jia, J. Ma, and L. Gan, "Radiometric identification based on low-rank representation and minimum prediction error regularization," *IEEE Commun. Lett.*, vol. 21, no. 8, pp. 1847–1850, Aug. 2017.
- [6] K. Merchant, S. Revay, G. Stantchev, and B. Noursain, "Deep learning for RF device fingerprinting in cognitive communication network," *IEEE J. Sel. Topics Signal Process.*, vol. 12, no. 1, pp. 160–167, Feb. 2018.
- [7] J. Wright, A. Y. Yang, A. Ganesh, S. Sastry, and Y. Ma, "Robust face recognition via sparse representation," *IEEE Trans. Pattern Anal. Mach. Intell.*, vol. 31, no. 2, pp. 210–227, Feb. 2009.
- [8] *Electromagnetic Compatibility and Radio Spectrum Matters (ERM); Digital Mobile Radio (DMR) Systems; Part 1: DMR Air Interface (AI) Protocol*, Standard ETSI TS 102 361-1, European Telecommun. Standards Inst., 2016.
- [9] A. M. Bruckstein, D. L. Donoho, and M. Elad, "From sparse solutions of systems of equations to sparse modeling of signals and images," *SIAM Rev.*, vol. 51, no. 1, pp. 34–81, Feb. 2009.
- [10] H. Abdi and L. J. Williams, "Principal component analysis," *Wiley Interdiscipl. Rev. Comput. Statist.*, vol. 2, no. 4, pp. 433–459, 2010.
- [11] S. S. Chen, D. L. Donoho, and M. A. Saunders, "Atomic decomposition by basis Pursuit," *SIAM Rev.*, vol. 43, no. 1, pp. 129–159, 2001.
- [12] L. Ding, S. Wang, F. Wang, and W. Zhang, "Specific emitter identification via convolutional neural networks," *IEEE Commun. Lett.*, vol. 22, no. 12, pp. 2591–2594, Dec. 2018.